Functional Analysis of the α-Defensin Disulfide Array in Mouse Cryptdin-4*

Atsuo Maemoto‡§, Xiaoqing Qu‡§, K. Johan Rosengren¶, Hiroki Tanabe‡‖, Agnes Henschen-Edman**, David J. Craik¶‡‡, and Andre J. Ouellette‡§§¶¶

*From the Departments of ‡Pathology, **Molecular Biology and Biochemistry, and §§Microbiology and Molecular Genetics, the College of Medicine and School of Biological Sciences, University of California, Irvine, California 92697-4800 and the ¶Institute for Molecular Bioscience, University of Queensland, Brisbane, Queensland 4072, Australia*

The α-defensin antimicrobial peptide family is defined by a unique tridisulfide array. To test whether this invariant structural feature determines α-defensin bactericidal activity, mouse cryptdin-4 (Crp4) tertiary structure was disrupted by pairs of site-directed Ala for Cys substitutions. In a series of Crp4 disulfide variants whose cysteine connectivities were confirmed using NMR spectroscopy and mass spectrometry, mutagenesis did not induce loss of function. To the contrary, the *in vitro* bactericidal activities of several Crp4 disulfide variants were equivalent to or greater than those of native Crp4. Mouse Paneth cell α-defensins require the proteolytic activation of precursors by matrix metalloproteinase-7 (MMP-7), prompting an analysis of the relative sensitivities of native and mutant Crp4 and proCrp4 molecules to degradation by MMP-7. Although native Crp4 and the α-defensin moiety of proCrp4 resisted proteolysis completely, all disulfide variants were degraded extensively by MMP-7. Crp4 bactericidal activity was eliminated by MMP-7 cleavage. Thus, rather than determining α-defensin bactericidal activity, the Crp4 disulfide arrangement confers essential protection from degradation by this critical activating proteinase.

The mammalian defensins comprise the α-, β-, and θ-defensin families of cationic, Cys-rich antimicrobial peptides, and each subfamily is characterized by a distinctive tridisulfide array (1). α-Defensins are cationic, amphipathic, 3–4-kDa peptides with a β-sheet polypeptide backbone and broad spectrum antimicrobial activities (1). The consensus α-defensin tertiary structure is established by six cysteines that are spaced in a pattern that facilitates the formation of invariant disulfide bonds between Cys^I-Cys^{VI}, Cys^{II}-Cys^{IV}, and Cys^{III}-Cys^V (2) (Fig. 1). These conserved α-defensin disulfide pairings have been inferred to have a role in determining, perhaps critically, the bactericidal activity of these peptides.

Paneth cell α-defensins confer enteric immunity (3) and, thus, knowledge of determinants of peptide activity and biosynthetic regulation will improve the understanding of the role of these α-defensins in mucosal immunity. For example, mouse Paneth cell α-defensins, termed cryptdins (Crps),[1] are secreted into the lumen of small intestinal crypts at concentrations of 25–100 mg/ml, four orders of magnitude greater than their minimum bactericidal concentrations (4). In mice, Paneth cell α-defensin precursors (proCrps) are processed to their biologically active forms by specific proteolytic cleavage events catalyzed by matrix metalloproteinase-7 (MMP-7, matrilysin). Disruption of the *MMP-7* gene abrogates proCrp activation, eliminating the accumulation of functional mature Crp peptides from the small intestine (5). Consequently, MMP-7-null mice have impaired enteric innate immunity in response to oral bacterial infection (5). Also, in mice transgenic for the human Paneth cell α-defensin HD5, the minitransgene is expressed specifically in Paneth cells, and the mice are immune to oral infection by virulent strains of *Salmonella enterica* serovar Typhimurium (serovar Typhimurium) (3).

Here, we report on the role of the disulfide array in the mouse Paneth cell α-defensin cryptdin-4 (Crp4) (6, 7). Paired Ala for Cys amino acid substitutions in Crp4 were tested for effects on bactericidal activity and resistance to the activating proteinase MMP-7. Mutations that disrupted disulfide bonds did not inactivate peptide bactericidal activity regardless of position. However, Crp4 and proCrp4 molecules with disrupted disulfides were proteolyzed extensively by MMP-7, disclosing a critical protective role for the disulfide array in peptide biosynthesis.

EXPERIMENTAL PROCEDURES

Preparation of Recombinant Crp4 Peptide Variants—Recombinant Crp4 peptides were expressed in *Escherichia coli* as N-terminal His_6-tagged fusion proteins from the EcoRI and SalI sites of the pET28a expression vector (Novagen, Inc., Madison, WI) as described (8, 9). The Crp4-coding cDNA sequences were amplified using the forward primer ER1-Met-C4-F (5′-GCGCGAATTCATCGAGGGAAGG<u>ATG</u>GGTTTGT-TATGCTATTGT-3′) paired with the reverse primer pMALCrp4-R (5′-ATATATGTCGACTCAGCGACAGCAGAGCGTGTACAATAAATG-3′) as reported previously (9). For proCrp4, the forward primer pETPCr4-F (5′-GCGCGAATTC<u>ATG</u>GATCCTATCCAA AACACA-3′) was paired with the reverse primer SLpMALCrp4R (5′-ATATATGTCGACTGT-TCAGCGGCGGGGGCAGCAGTACAA-3′), corresponding to nucleotides 104–119 and 301–327 in preproCrp4 cDNA (8). The underlined codons in the forward primers denote Met codons introduced upstream

[1] The abbreviations used are: Crp, cryptdin; proCrp, pro-cryptdin (Paneth cell α-defensin precursor); MMP-7, matrix metalloproteinase-7 or matrilysin; serovar Typhimurium, *Salmonella enterica* serovar Typhimurium; RP-HPLC, reverse-phase high performance liquid chromatography; MALDI-TOF MS, matrix-assisted laser desorption ionization mode mass spectrometry; AU-PAGE, acid-urea PAGE; CFU, colony-forming unit; PIPES, 1,4-piperazinediethanesulfonic acid.
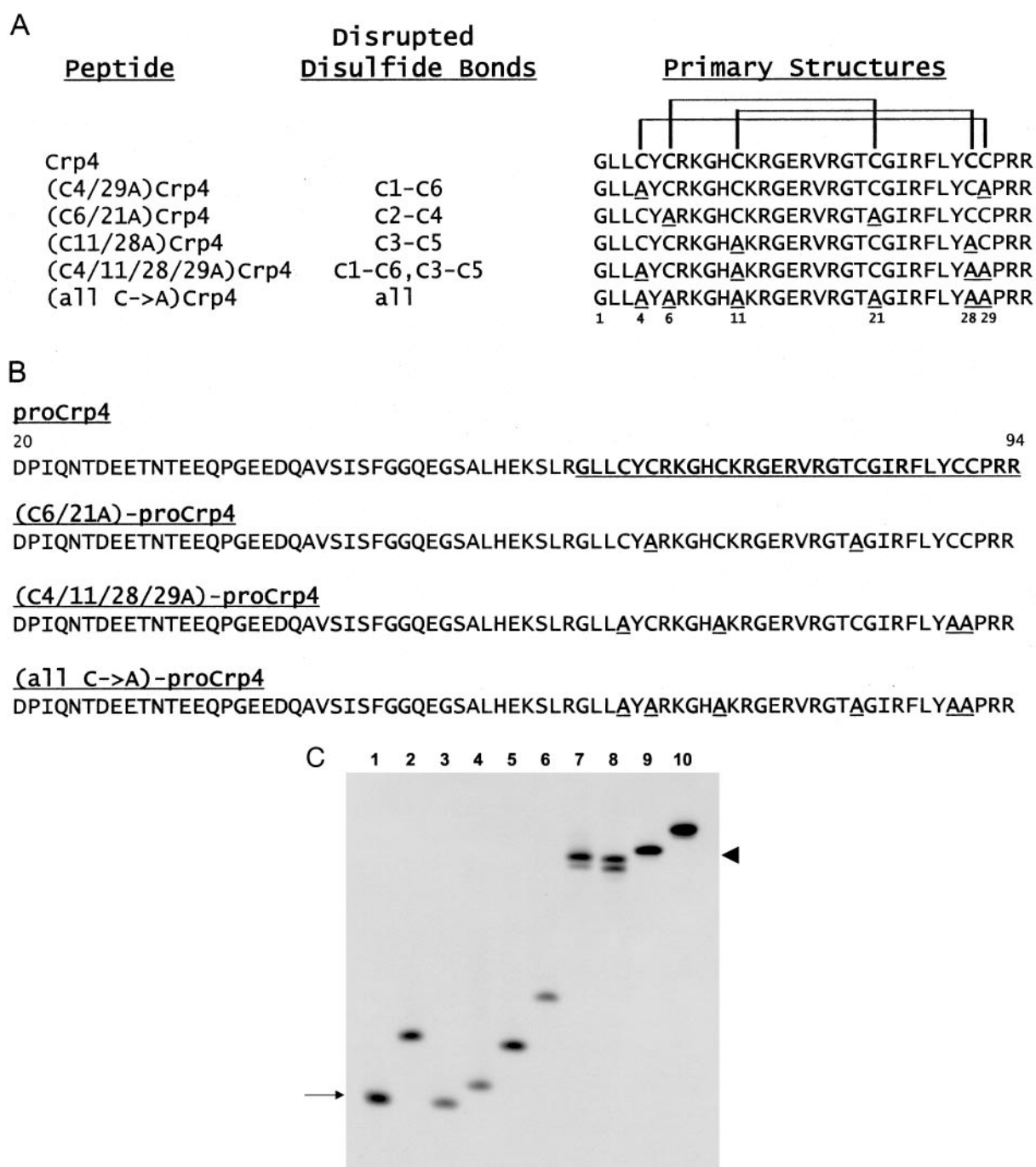
A

Peptide	Disrupted Disulfide Bonds	Primary Structures

Primary Structures (with disulfide bonds shown):

```
                                          ┌────────┬──────┬────────┬──────┐
                                          │    ┌───┼──────┤        │      │
                             GLLCYCRKGHCKRGERVRGTCGIRFLYCCPRR
```

Peptide	Disrupted Disulfide Bonds	Primary Structures
Crp4		GLLCYCRKGHCKRGERVRGTCGIRFLYCCPRR
(C4/29A)Crp4	C1-C6	GLLAYCRKGHCKRGERVRGTCGIRFLYCAPRR
(C6/21A)Crp4	C2-C4	GLLCYARKGHCKRGERVRGTAGIRFLYCCPRR
(C11/28A)Crp4	C3-C5	GLLCYCRKGHAKRGERVRGTCGIRFLYACPRR
(C4/11/28/29A)Crp4	C1-C6,C3-C5	GLLAYCRKGHAKRGERVRGTCGIRFLYAAPRR
(all C->A)Crp4	all	GLLAYARKGHAKRGERVRGTAGIRFLYAAPRR

Residue positions: 1 4 6   11   21   28 29

B

proCrp4
20   94

DPIQNTDEETNTEEQPGEEDQAVSISFGGQEGSALHEKSLR**GLLCYCRKGHCKRGERVRGTCGIRFLYCCPRR**

(C6/21A)-proCrp4

DPIQNTDEETNTEEQPGEEDQAVSISFGGQEGSALHEKSLRGLLCY**A**RKGHCKRGERVRGT**A**GIRFLYCCPRR

(C4/11/28/29A)-proCrp4

DPIQNTDEETNTEEQPGEEDQAVSISFGGQEGSALHEKSLRGLL**A**YCRKGH**A**KRGERVRGTCGIRFLY**AA**PRR

(all C->A)-proCrp4

DPIQNTDEETNTEEQPGEEDQAVSISFGGQEGSALHEKSLRGLL**A**Y**A**RKGH**A**KRGERVRGT**A**GIRFLY**AA**PRR

C 1 2 3 4 5 6 7 8 9 10

Fig. 1. **Recombinant Crp4 and proCrp4 disulfide variants.** The primary structures of recombinant Crp4 and proCrp4-(20–94) peptides prepared and investigated in these studies are aligned in *panels A* and *B*, respectively. Numerals above the Crp4 sequence refer to residue positions in reference to the N-terminal Gly of native Crp4 as residue position number 1. Altered Cys to Ala mutations in Crp4 and proCrp4 peptide variants are shown in *underlined*, *boldfaced text*. Multiple mutation designations used in *panels A* and *B* are as follows: *C4/29A*, C4A/C29A; *C6/21A*, C6A/C29A; *C11/28A*, C11A/C28A; *C4/11/28/29A*, C4A/C11A/C28A/C29A; all *C→A*, C4A/C6A/C11A/C21A/C28A/C29A. The disulfide bond designations used in *panel A* are as follows: *C1-C6*, Cys^I-Cys^{VI}; *C2-C4*, Cys^{II}-Cys^{IV}; *C3-C5*, Cys^{III}-Cys^V. In *panel C*, 3-μg samples of purified recombinant Crp4 and variants of Crp4 and 6-μg samples of proCrp4 and variants were resolved by AU-PAGE and stained with Coomassie Blue. *Lane 1*, Crp4 (*lower left arrow*); *lane 2*, (C4A/C29A)-Crp4; *lane 3*, (C6A/C21A)-Crp4; *lane 4*, (C11A/C28A)-Crp4; *lane 5*, (C4A/C11A/C28A/C29A)-Crp4; *lane 6*, (C4A/C6A/C11A/C21A/C28A/C29A)-Crp4; *lane 7*, proCrp4 (*upper right arrowhead*); *lane 8*, (C6/21)-proCrp4; *lane 9*, (C4/11/28/29)-proCrp4; *lane 10*, (C4A/C6A/C11A/C21A/C28A/C29A)-proCrp4.

of each peptide N terminus to provide a CNBr cleavage site (8, 9). In all instances, reactions were performed using the GeneAmp PCR Core Reagents (Applied Biosystems, Foster City, CA) by incubating the reaction mixture at 94 °C for 5 min followed by successive cycles at 94 °C for 30 s, 60 °C for 30 s, and 72 °C for 30 s for 30 cycles and then a final extension reaction at 72 °C for 7 min.

Mutagenesis at Cys Residue Positions—Mutations were introduced into Crp4 by PCR as described previously (8) in the order described below. In the first round of mutagenesis the Crp4 construct in pET-28a (9) was used as template. In PCR reaction number 1, a mutant forward

primer, *e.g.* Crp4-C11A-F, containing the mutation for peptide residue position 11 flanked by three natural codons was paired with the reverse primer T7 terminator (Invitrogen), a downstream sequencing primer in the pET-28a vector. In PCR reaction number 2, the mutant reverse primer Crp4-C11A-R, the reverse complement of the mutant forward primer, was paired with the T7 promoter forward primer, again from the pET-28a. After amplification at 94 °C for 5 min followed by successive cycles at 94 °C for 30 s, 60 °C for 30 s, and 72 °C for 30 s for 30 cycles and then a final extension reaction at 72 °C for 7 min, samples of purified products from reactions number 1 and number 2 were com-
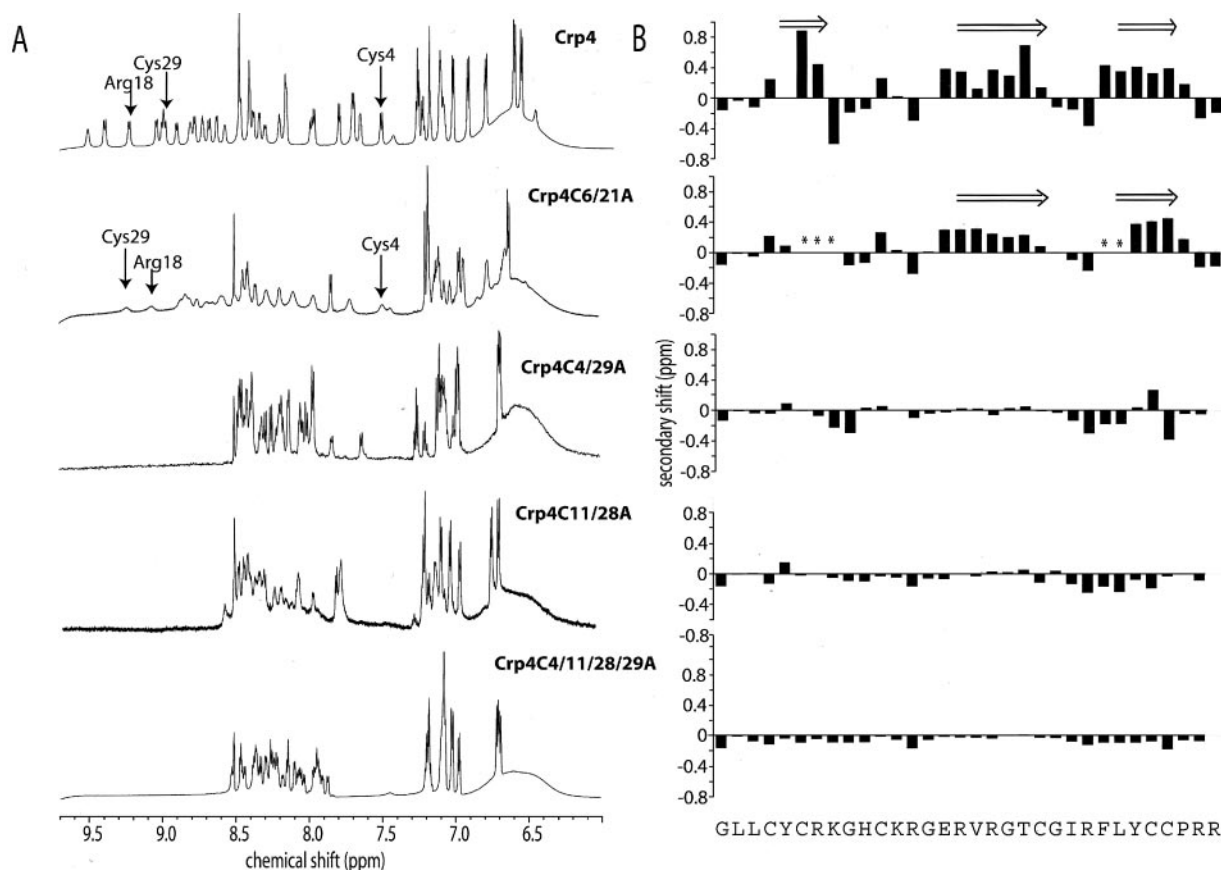
FIG. 2. **NMR characterization of Crp4 and disulfide mutants.** *Panel A* shows the amide region of the one-dimensional spectra. Selected upfield (Cys[4]) and downfield (Arg[18] and Cys[29]) NH signals are labeled for native Crp4 and (C6A/C21A)-Crp4 (*Crp4C6/21A*), illustrating the excellent signal dispersion characteristic of folded proteins. *Panel B* shows αH secondary shifts for each residue in the native and disulfide deficient peptides. *Arrows* indicate regions of the β-sheet previously identified in the solution structure of a typical α-defensin, RK-1 (23). Native Crp4 and (C6A/C21A)-Crp4 display stretches of consecutive αH secondary shifts with values >0.1 ppm in these regions, strongly indicating that the β-sheet structural elements are also present in these two peptides. By contrast the other mutants have poor dispersion and αH secondary shifts typically < 0.1 ppm, indicative of random coil structure. The *asterisks* indicate residues whose NH signals are broadened beyond detection in the spectrum of (C6A/C21A)-Crp4. *Crp4C4/29A*, (C4A/C29A)-Crp4; *Crp4C11/28A*, (C11A/C28A)-Crp4; *Crp4C4/11/28/29A*, (C4A/C11A/C28A/C29A)-Crp4.

bined as templates in PCR reaction number 3 using the T7 promoter and terminator primers as amplimers. All mutated Crp4 templates were cloned in pCR-2.1 TOPO, verified by DNA sequencing, excised with SalI and EcoRI, subcloned into pET28a plasmid DNA (Novagen, Inc.), and transformed into *E. coli* BL21(DE3)-CodonPlus-RIL cells (Stratagene) for recombinant expression. The underlined codons in the forward primers denote Met codons introduced upstream of each peptide N terminus to provide a CNBr cleavage site (8, 9).

Mutant Crp4 peptides with additional Ala for Cys substitutions were prepared by accumulating mutations in modified templates as follows. For (C11A)-Crp4, the pET28-Crp4 construct was used as the template in reaction number 1 with the forward primer Crp4-C11A-F (5′-AAAG-GACAC**GCC**AAAAGAGGA-3′) and the reverse primer Crp4-C11A-R (5′-TCCTCTTTT**GGC**GTGTCCTTT-3′) paired with the T7 promoter and the terminator primers (pET T7 primers), with samples of these products used as a combined template for full-length product amplification with pET T7 primers. For (C21A)-Crp4, the pET28-Crp4 construct template was amplified with the Crp4-C21A-F forward primer (5′-CGTGGGACT**GCT**GGAATACGA-3′) and the Crp4-C21A-R reverse primer (5′-TCGTATTCC**AGC**AGTCCCACG-3′) paired with the pET T7 primers, and the final products were prepared as described above. For (C11A/C21A)-Crp4, the full-length (C11A)-Crp4 amplification product was amplified with Crp4-C21A-F and Crp4-C21A-R and the pET T7 primers as described above. For (C6A/C21A)-Crp4, the full-length (C21A)-Crp4 product was amplified with the Crp4-C6A-F forward primer (5′-GAATTCATGGGGTTTGTTATGCTAT**GCT**AGA-3′) paired with pMALCrp4-R. For (C11A/C28A)-Crp4, the full-length (C11A)-Crp4 product was amplified with the Crp4-C28A-R reverse primer (5′-GTC-GACTCATCAGCGGCGGGGACA**GGC**GTA-3′) to amplify the full-length product. To prepare (C4A/C29A)-Crp4, the Crp4-coding pET28a was amplified using the Crp4-C4A-F forward primer (5′-ACACAC-

GAATTCATGGGGTTTGTTA**GCC**TATTGT-3′) and the Crp4-C29A-R reverse primer (5′-ACACACGTCGACTCATCAGCGGCGGGG**TGC**GCA-3′). For (C4A/C11A/C28A/C29A)-Crp4, the full-length (C11A)-Crp4 amplification product was used as the template with the Crp4-C4A-F forward primer and the Crp4-C28AC29A-R reverse primer (5′-GTC-GACTCATCAGCGGCGGGG**TGCGGC**GTA-3′). To mutagenize all Cys positions in Crp4 (Cys[4], Cys[6], Cys[11], Cys[21], Cys[28], and Cys[29]) the full-length (C11A/C21A)-Crp4 PCR product was amplified with the Crp4-C4AC6A-F forward primer (5′-GAATTCATGGGGTTTGTTA**GCC**TAT-**GCT**AGA-3′) and the Crp4-C28AC29A-R reverse primer. Boldfaced residues in the primer sequences above denote codons for alanines.

To prepare (C4A/C11A/C28A/C29A)-proCrp4 and (C4A/C6A/C11A/C21A/C28A/C29A)-proCrp4, the peptide-coding regions of the (C4A/C11A/C28A/C29A)- and (C4A/C6A/C11A/C21A/C28A/C29A)-Crp4 pET28 constructs were amplified with the PC4Cod54/63-F forward primer (5′-CTTCATGAAAAATCTTTGAGAGGTTTGTTA-3′) and the Crp4-C28AC29A-R reverse primer, and the proCrp4 prosegment coding region was amplified from a proCrp4 pET-28a construct (8) using the pETPCr4-F forward primer (5′-GCGCGAATTC<u>ATG</u>GATCCTATC-CAAAACACA-3′) with the PC4Cod54/63-R reverse primer (5′-TAACAAACCTCTCAAAGATTTTTCATGAAG-3′). The underlined codon in the forward primer denotes a Met codon introduced upstream of the peptide N terminus to provide a CNBr cleavage site (8, 9). Samples of these reactions were used as a combined template with pETPCr4-F and Crp4-C28AC29A-R to prepare the full-length proCrp4 molecules with mutated disulfide bonds.

Purification of Recombinant Crp4 Proteins—Recombinant proteins were expressed and purified as His-tagged Crp4 fusion peptides as described (8). Briefly, recombinant proteins were expressed at 37 °C in Terrific Broth medium by induction with 0.1 mM isopropyl-β-D-1-thio-galactopyranoside for 6 h at 37 °C, cells were lysed by sonication in 6 M
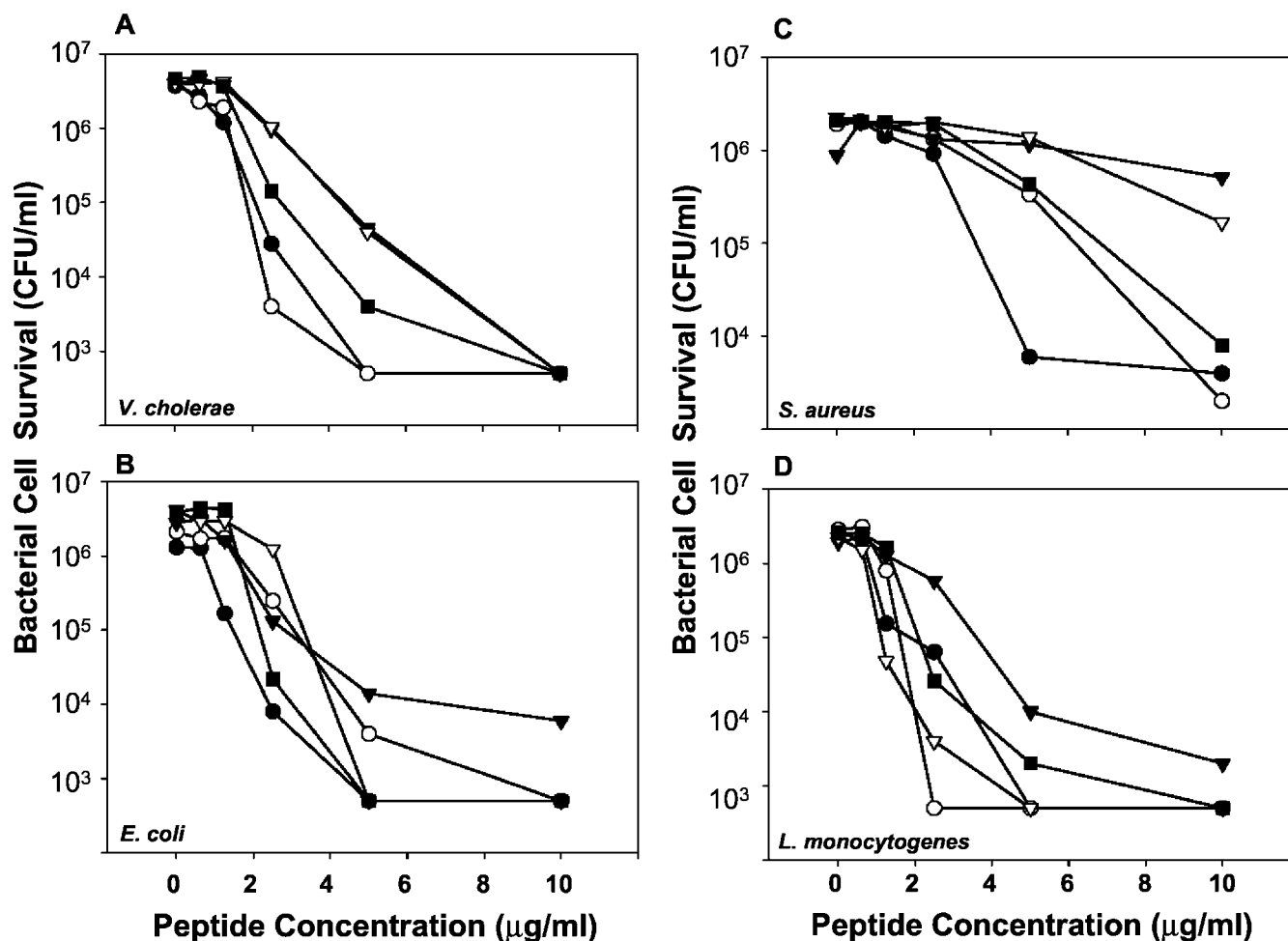
FIG. 3. **Crp4 disulfide variants are bactericidal.** Exponentially growing *V. cholerae* (*A*), *E. coli* ML 35 (*B*), *S. aureus* (*C*), and *L. monocytogenes* (*D*) were exposed to the peptide concentrations shown in 50 μl of 10 mM PIPES (pH 7.4) and 1% trypticase soy broth for 1 h at 37 °C (see "Experimental Procedures"). Following exposure, bacteria were plated on semi-solid media and incubated for 16 h at 37 °C. Surviving bacteria were quantitated (CFU/ml) for each peptide concentration. Bacterial counts below 1×10^3 CFU/ml indicate that no surviving colonies were detected. Symbols are as follows: ●, Crp4; ▼, (C6A/C21A)-Crp4; ▽, (C11A/C28A)-Crp4; ○, (C4A/C11A/C28A/C29A)-Crp4; and ■, (C4A/C6A/C11A/C21A/C28A/C29A)-Crp4.

guanidine-HCl in 100 mM Tris-Cl (pH 8.1), and the soluble protein fraction was clarified by centrifugation (8–10). His-tagged Crp4 fusion peptides were purified using nickel-nitrilotriacetic acid (Qiagen) resin affinity chromatography (8). After CNBr cleavage, Crp4 peptides were purified by C18 reverse-phase high performance liquid chromatography (RP-HPLC) and quantitated by bicinchoninic acid (Pierce), and the molecular masses of the purified peptides were determined using matrix-assisted laser desorption ionization mode mass spectrometry (Voyager-DE MALDI-TOF, PE-Biosystems, Foster City, CA) in the Mass Spectroscopy Facility, Department of Chemistry, University of California, Irvine, CA.

NMR Spectroscopy—Samples of Crp4 and the mutants used for NMR analysis contained 2 mg of Crp4, 0.6 mg of (C6A/C21A)-Crp4, and <0.3 mg of the other mutants dissolved in 0.5 ml of 95% H_2O/5% D_2O at pH 4. One-dimensional and two-dimensional total correlation spectroscopy with a MLEV17 mixing time of 80 ms and two-dimensional nuclear Overhauser effect spectroscopy spectra with a mixing time of 200 ms were recorded for all analogues on a Bruker DMX 750 MHz spectrometer at 298 K. In all experiments, the carrier frequency was set at the center of the spectrum on the solvent signal, and all spectra were recorded in phase-sensitive mode using the time-proportional phase increment method. Solvent suppression was achieved by a modified WATERGATE sequence. Two-dimensional spectra collected with >4000 data points in the f2 dimension and 512 increments on the f1 dimension over a spectral width corresponding to 12 ppm. Resonance assignments were achieved by standard sequential assignment strategies (11).

Bactericidal Peptide Assays—Recombinant peptides were tested for microbicidal activity against *E. coli* ML35, wild-type serovar Typhimurium strains CS022, JSG210, and 14082 (from Dr. Samuel I. Miller,

University of Washington), *Vibrio cholerae, Staphylococcus aureus* 710a, and *Listeria monocytogenes* 104035 as described (12). Bacteria (~5×10^6 colony forming units (CFU) per milliliter), resuspended in 10 mM PIPES (pH 7.4) supplemented with 0.01 volume of trypticase soy broth, were incubated with test peptides in 50 μl for 1 h at 37 °C, and surviving bacteria were counted (CFU/ml) after overnight growth on semi-solid media (8, 9).

Cleavage of Crp4 and proCrp4 Disulfide Variants with MMP-7 in Vitro—Recombinant Crp4, proCrp4, and variants with site-directed mutations in the disulfide array were digested with MMP-7 and analyzed for proteolysis by AU-PAGE, and samples of the proteolytic digests were tested in bactericidal peptide assays and analyzed by N-terminal sequencing by Edman degradation as described (8). Samples (11 μg) of proCrp4 and all proCrp4 variants, as well as 5-μg samples of Crp4 and variants, were incubated with an activated recombinant human MMP-7 (0.3~1.0 μg) catalytic domain (Calbiochem, La Jolla, CA) in buffer containing 10 mM HEPES (pH 7.4), 150 mM NaCl, and 5 mM $CaCl_2$ for 18–24 h at 37 °C (8). Equimolar samples of all digests were analyzed by AU-PAGE, and 3-μg quantities of complete digests were subjected to five or more cycles of Edman degradation in the University of California, Irvine Biomedical Protein and Mass Spectrometry Resource Facility.

The biological effects of MMP-7-mediated proteolysis of Crp4 molecules with mutations in the disulfide array was assayed by conducting bactericidal peptide assays as above. Bacterial target cells consisting of exponentially growing bacteria (~1×10^6 CFU/ml) were incubated with equimolar quantities (0 to 20 μg/ml) of Crp4 or pro-Crp4 peptide variants that had been incubated overnight at 37 °C with or without MMP-7.

Role of the α-Defensin Disulfide Array

RESULTS

Mutagenesis of the Crp4 Disulfide Array—Recombinant Crp4 variants with site-directed mutations in the tridisulfide array (Fig. 1*A*) were prepared by expression in *E. coli* using the pET-28 vector system (8). As shown in Fig. 1, Crp4 variants included molecules null for the following: (*a*) individual Cys^I-Cys^{VI}, $Cys^{II}-Cys^{IV}$, or $Cys^{III}-Cys^V$ disulfides; (*b*) both the Cys^I-Cys^{VI} and $Cys^{III}-Cys^V$ bonds; and (*c*) a Crp4 peptide with all Cys residues converted to Ala and, thus, disulfide-null. All variant Crp4 peptides were purified to homogeneity by RP-HPLC as verified by analytical RP-HPLC (not shown) and AU-PAGE analyses in which the peptides migrated as expected relative to native Crp4 (Fig. 1*C*) (8). Alkylation of α-defensins disrupts β-sheet structure, linearizing the molecule and reducing its mobility in AU-PAGE (13). Similarly, the mobility of these variant Crp4 molecules was diminished with increased numbers of disrupted disulfides (Fig. 1*C*).

A series of one-dimensional and two-dimensional total correlation spectroscopy and nuclear Overhauser effect spectroscopy NMR spectra was recorded to assess the structural integrity of recombinant Crp4 and the disulfide-deficient variants. The two-dimensional spectra were sequentially assigned and used to derive chemical shifts for the backbone protons, which are a sensitive monitor of structure as summarized in Fig. 2. Native Crp4 and the C6A/C21A variant have widely dispersed amide signals characteristic of well folded peptides (Fig. 2*A*). On the other hand, the amide signals for the C4A/C29A, C11A/C28A, and C4A/C11A/C28A/C29A variants have a narrow amide dispersion typical of random coil conformations. Confirmation that the native peptide and the C6A/C21A variant are well folded and that the other variants are not is evident from the αH secondary shifts (Fig. 2*B*), *i.e.* the differences between the observed chemical shifts of a given amino acid and those for the corresponding residue in a random coil peptide. The presence of several consecutive residues with positive αH secondary shifts of magnitude >0.1 ppm provides a strong indication of β-strand structure. Such regions are seen in Crp4 and in the C6A/C21A mutant and correspond to the regions comprising a triple-stranded β-sheet typically seen in other α-defensins (Fig. 2*B*, *arrows*). By contrast, the C4A/C29A, C11A/C28A, and C4A/C11A/C28A/C29A Crp4 mutants have small secondary shifts characteristic of random coil peptides. These trends correspond well with the gel migration data in Fig. 1*C*, where the C6A/C21A variant migrates similarly to the native peptide, but the others have diminished mobility as would be expected for disordered peptides.

The α-Defensin Disulfide Array Does Not Determine Crp4 Bactericidal Activity in Vitro—To investigate the role of the Crp4 disulfide array, we assayed the *in vitro* bactericidal activities of Crp4 disulfide mutants against several bacterial species in relation to native Crp4 (Fig. 3). The overall bactericidal activities of Crp4 and Cys → Ala Crp4 variants were similar, although not identical, with all of the peptides reducing bacterial cell survival by at least 1000-fold at concentrations at or below 25 µg/ml (Figs. 3 and 4 and data not shown). Because differences in peptide bactericidal activities become more apparent in assays against species with inherently lower antimicrobial peptide sensitivities, the peptides were tested against strains of wild-type serovar Typhimurium, which has low α-defensin susceptibility relative to other species of bacteria (14–17). Three disulfide mutants, the C6A/C21A, C4A/C11A/C28A/C29A, and C4A/C6A/C11A/C21A/C28A/C29A variants of Crp4, were consistently more active than native Crp4 against wild-type serovar Typhimurium (Fig. 4). Therefore, Crp4 bactericidal activity is independent of disulfide mutagenesis with molecules lacking
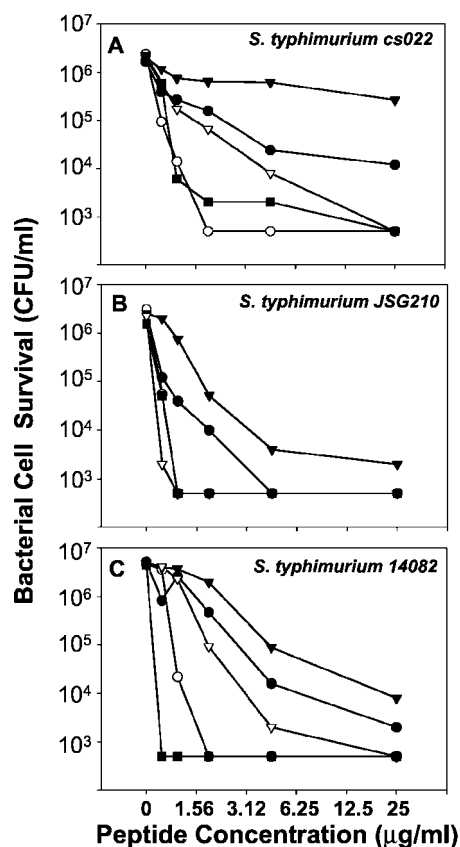

FIG. 4. **Bactericidal activity of Crp4 and Crp4 disulfide variants against serovar Typhimurium.** Exponentially growing wild-type serovar Typhimurium strains CS022 (*A*), JSG210 (*B*), and 14082 (*C*) were exposed to the peptides, and the surviving bacterial cells were quantitated (CFU/ml) (Fig. 3). Symbols are as follows: ●, Crp4; ▼, (C6A/C21A)-Crp4; ▽, (C11A/C28A)-Crp4; ○, (C4A/C11A/C28A/C29A)-Crp4; and ■, (C4A/C6A/C11A/C21A/C28A/C29A)-Crp4. Note that the (C4A/C11A/C28A/C29A)-Crp4 and (C4A/C6A/C11A/C21A/C28A/C29A)-Crp4 variants are more bactericidal against this generally defensin-resistant species.

more than one disulfide bond showing enhanced microbicidal activities, although the dose-response curves of certain peptides varied modestly (Figs. 3 and 4). Because mutagenesis at Crp4 disulfides did not induce loss of function, we considered alternative roles for the disulfide array, including protection of the peptide from degradation by the activating proteinase.

Disulfide Bonds Protect Crp4 from Proteolysis by MMP-7—Production of functional mouse Paneth cell α-defensins requires that MMP-7 mediate proteolytic cleavage of inactive proCrps (5). To test whether the disulfide array protects the Crp4 moiety from MMP-7 proteolysis during activation, we first assayed for cleavage products of native and mutant Crp4 molecules exposed to MMP-7 (Fig. 5). As reported previously (8), native Crp4 was completely resistant to MMP-7 *in vitro*, but all Crp4 peptides with disrupted cystine pairings were degraded extensively (Fig. 5*A*). As expected, MMP-7 activated native proCrp4 as shown by AU-PAGE analyses (Fig. 5*A*) and in functional assays (Fig. 6*A*, and see below). Consistent with peptide structures, the major degradation products detected on the gels (Fig. 5*A*) all have increased mobilities relative to the uncleaved disulfide-deficient peptide, except for (C6A/C21A)-Crp4. Its high intrinsic mobility is due to the loss of native-like globular structure on proteolysis, whereas the degradation products of the other, random coil peptide variants increased in mobility.

N-terminal sequencing of MMP-7 peptide digests detected four major cleavage sites in peptides lacking one disulfide bond,

A

FIG. 5. **MMP-7 degrades Crp4 variants with disrupted disulfide arrays.** Samples of Crp4 (5 μg), proCrp4 (11 μg), and Crp4 disulfide variants were incubated overnight at 37 °C in the presence or absence of MMP-7, the proCrp-activating enzyme. In *panel A*, 5-μg samples of the peptides shown were incubated with (+) or without (−) MMP-7, subjected to analytical AU-PAGE, and stained with Coomassie Blue (see "Experimental Procedures"). *Upper arrow* denotes proCrp4, and *lower arrow* denotes Crp4. Stained MMP-7 is evident below the positive (+) symbols near the gel origins. *C4/C29A*, (C4A/C29A)-Crp4; *C6/21A*, (C6A/C21A)-Crp4; *C11/28A*, (C11A/C28A)-Crp4; *C4/11/28/29A*, (C4A/C11A/C28A/C29A)-Crp4; *6C/A*, (C4A/C6A/C11A/C21A/C28A/C29A)-Crp4. In *panel B*, samples of Crp4 and Crp4 variants (3 μg) incubated overnight with 0.5-mol equivalents of MMP-7 (*panel A*) were analyzed by five cycles of N-terminal peptide sequencing. The primary cleavage sites disclosed by protein sequencing are noted by *inverted triangles* (▼) that interrupt the individual sequences, and the N termini detected at lower levels are depicted by *downward arrows* (↓). The characteristic α-defensin cysteine connectivities are shown in Crp4 and the mutant peptides. Positions at which Cys to Ala mutations occur are shown in *boldfaced type*. Note that MMP-7 does not cleave native Crp4; cleavage of native proCrp4 occurred as characterized previously (8). *(C6/21A)Crp4*, (C6A/C21A)-Crp4; *(C11/28A)Crp4*, (C11A/C28A)-Crp4; *(C4/11/28/29A)Crp4*, (C4A/C11A/C28A/C29A)-Crp4; *(all C→A)Crp4*, (C4A/C6A/C11A/C21A/C28A/C29A)-Crp4.

B
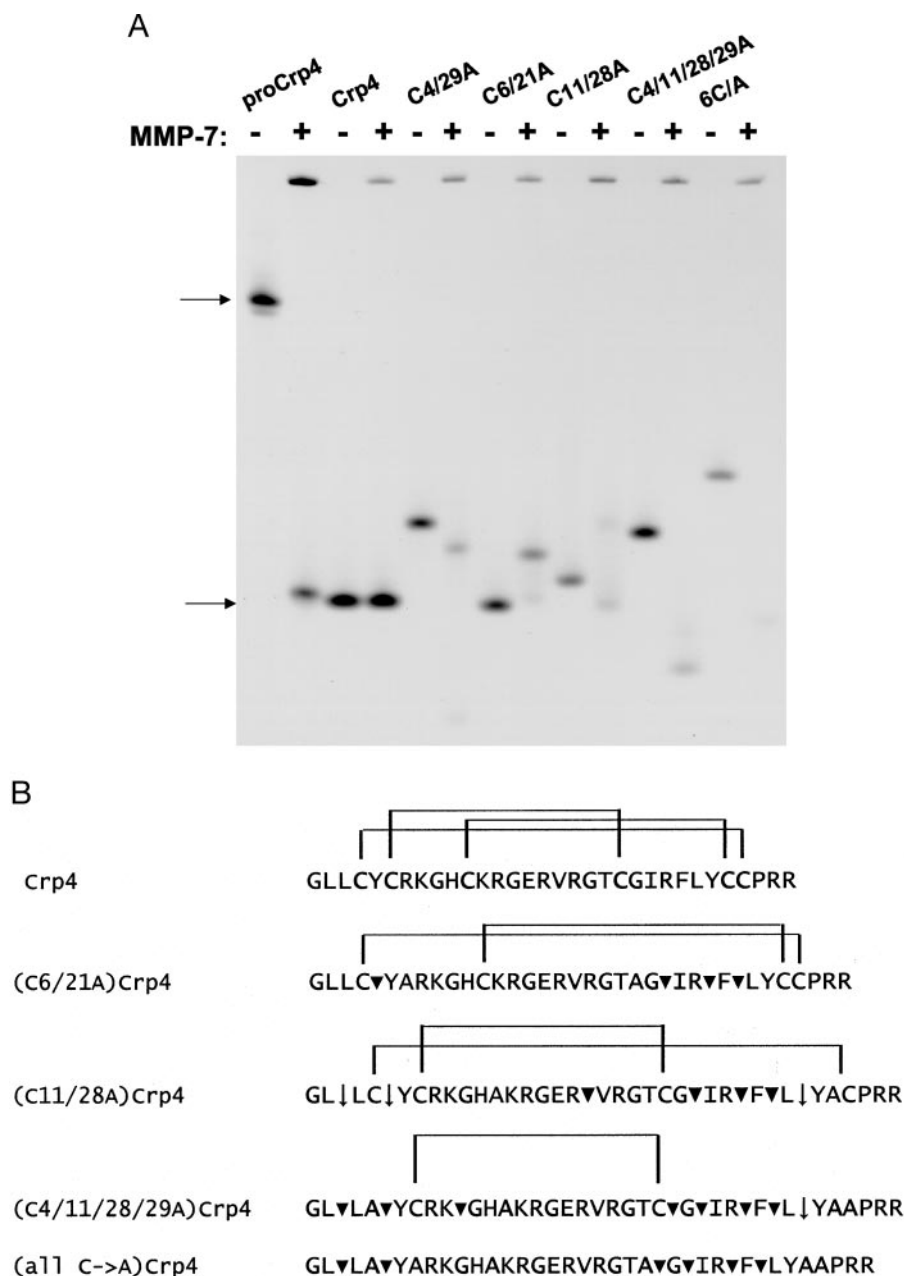
seven sites in (C4A/C11A/C28A/C29A)-Crp4, and six in (C4A/C6A/C11A/C21A/C28A/C29A)-Crp4 (Fig 5*B*), showing that the Crp4 disulfide array provided protection against proteolytic degradation. (C4A/29A)-Crp4 also was cleaved by MMP-7 as judged by its AU-PAGE mobility after enzyme treatment (Fig. 5*A*), but C4A/C29A peptide digests were not sequenced. MALDI-TOF MS analysis of MMP-7 digests of (C4A/C29A)-Crp4 identified peptide masses of 1868.2, 3342.9, and 3527.2 that are consistent with cleavage events at $Leu^2 \downarrow Leu^3$, $Ala^4 \downarrow Tyr^5$, and $Arg^{16} \downarrow Val^{17}$. Although cleavage at these sites is evident, we cannot exclude the possibility of additional cleavage sites in (C4A/C29A)-Crp4 that were not detected by this approach. Thus, a predicted outcome of α-defensin disulfide mutagenesis *in vivo* would be peptide degradation during precursor activation.

Proteolysis of Crp4 Disulfide Variants Abolishes Bactericidal Activity—The bactericidal activities of (C4/11/28/29/A)-Crp4 and (C4A/C6A/C11A/C21A/C28A/C29A)-Crp4 were eliminated by proteolysis with MMP-7. (C6A/C21A)-Crp4 and (C11A/C28A)-Crp4 containing Cys^I-Cys^{VI} plus Cys^{III}-Cys^V and Cys^I-Cys^{VI} plus Cys^{II}-Cys^{IV} connectivities, respectively, were digested extensively by MMP-7 (Fig. 5*B*), yet the cleaved peptides retained activity similar to that of native Crp4 (Fig. 6*B*). Thus, certain proteolytic fragments of these Crp4 variants are bactericidal despite the hydrolysis of four peptide bonds. In the preliminary RP-HPLC of MMP-7-digested (C11A/C28A)-Crp4 separations, bactericidal activity was isolated in a single fraction coinciding with a prominent HPLC peak containing peptide fragments with masses of 3125, 2249, and 878 atomic mass units. When combined with N-terminal sequence analysis of those fractions (not shown), we deduced that the active fraction consisted of two Crp4 fragments, Leu^3–Gly^{22} (2250.6 atomic mass units) and Leu^{26}–Arg^{32} (878.0 atomic mass units) joined by the C^I-C^{VI} disulfide bond to give a mass of 3125 (not shown). As before (8, 9), MMP-7 activated native proCrp4 (Fig. 6*A*) and did not affect Crp4 bactericidal activity as its MMP-7 resistance predicted (Fig. 6*A*, and see Fig. 5). In contrast, proteolysis of (C4A/C11A/C28A/C29A)-Crp4 and (C4A/C6A/C11A/C21A/C28A/C29A)-Crp4 by MMP-7 (Fig. 5*B*) abolished *in vitro* bactericidal activity (Fig. 6*C*, *open symbols*). These results show
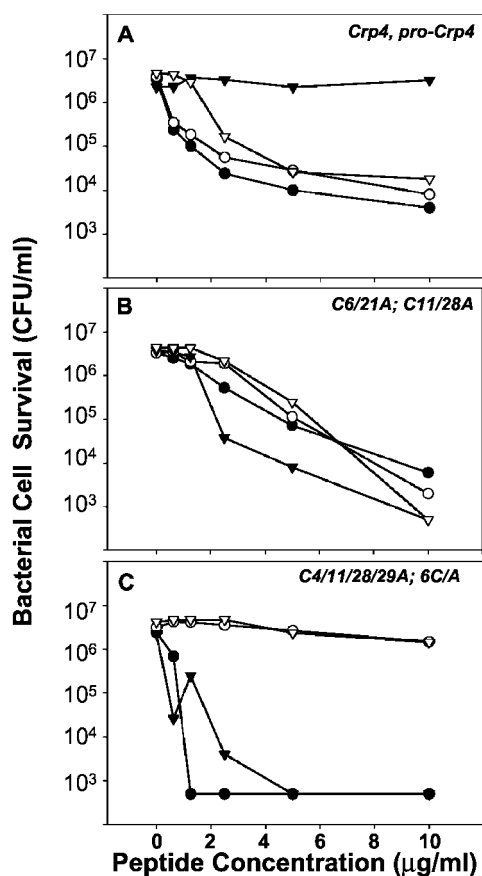
Role of the α-Defensin Disulfide Array

FIG. 6. **MMP-7-mediated proteolysis abolishes the bactericidal activity of Crp4 disulfide mutants.** Equimolar quantities of Crp4, proCrp4, and Crp4 disulfide variants were incubated overnight at 37 °C in the presence or absence of 0.5-mol quantities of MMP-7, and equimolar quantities of all digests were assayed for bactericidal activity against *L. monocytogenes*. In all panels, *filled symbols* denote samples not incubated with MMP-7, and *open symbols* denote samples exposed to MMP-7. *A*, ●, Crp4 without MMP-7; ○, Crp4 with MMP-7; ▼, proCrp4 without MMP-7; and ▽, proCrp4 with MMP7. *B*, ●, (C6A/C21A)-Crp4 (*C6/21A*) without MMP-7; ○, (C6A/C21A)-Crp4 (*C6/21A*) with MMP-7; ▼, (C11A/C28A)-Crp4 (*C11/28A*) without MMP-7; ▽, (C11A/C28A)-Crp4 (*C11/28A*) with MMP-7. *C*, ●, (C4A/C11A/C28A/C29A)-Crp4 (*C4/11/28/29A*) without MMP-7; ○, (C4/11/28/29)-Crp4 (*C4/11/28/29A*) with MMP-7; ▼, (C4A/C6A/C11A/C21A/C28A/C29A)-Crp4 (*6CA*) without MMP-7; ▽, (C4A/C6A/C11A/C21A/C28A/C29A)-Crp4 (*6CA*) with MMP-7. Note that MMP-7 proteolysis eliminates the bactericidal activity of (C4/11/28/29)-Crp4 and (C4A/C6A/C11A/C21A/C28A/C29A)-Crp4.

that Crp4 *in vitro* bactericidal activity is independent of the disulfide array and that tertiary structure protects Crp4 from proteolysis that would destroy its activity. To evaluate that possibility more directly in the context of the biosynthetic pathway, we analyzed the proteolytic stability of proCrp4 mutants with disrupted disulfide arrays (Fig. 1*B*) in *in vitro* activation reactions catalyzed by MMP-7.

Disulfide Bonds Protect the proCrp4 α-Defensin Region from Degradation by MMP-7—To test whether the α-defensin disulfide array protects against MMP-7-mediated proteolysis of the Crp4 precursor, three proCrp4 molecules with paired Ala for Cys substitutions (Fig. 1*B*) were prepared and exposed to MMP-7 (Fig. 7). When native proCrp4 was incubated with MMP-7 as before, the Crp4 peptide region of the precursor was protected fully during *in vitro* activation (Fig. 7, *A* and *B*). On the other hand, (C6A/C21A)-, (C4A/C11A/C28A/C29A)-, and (C4A/C6A/C11A/C21A/C28A/C29A)-proCrp4 were degraded by MMP-7 as evident by the nearly complete absence of processing products comigrating with Crp4 (Fig. 7*A*) and the detection of

four cleavage sites within the defensin moiety (Fig 7*B*). Processing events at Ser[43] ↓ Ile[44], Ala[53] ↓ Leu[54], and Ser[58] ↓ Leu[59] (8) occurred normally in the proCrp4 proregion (Fig. 7*B*) regardless of the status of the disulfide array, although differences in the kinetics of MMP-7 processing of proCrp4 mutants is a possibility. AU-PAGE analysis suggested that (C6A/C21A)-proCrp4 was less extensively degraded, but N-terminal sequencing of digests showed that it was cleaved at the same sites as (C4A/C6A/C11A/C21A/C28A/C29A)-proCrp4 (Fig 7*B*), namely at Leu[62] ↓ Leu[63], Cys[64] ↓ Tyr[65], Gly[84] ↓ Ile[85], and Phe[87] ↓ Leu[88]. Except for cleavage at Gly[84] ↓ Ile[85], MMP-7 digestion of disulfide-deficient and alkylated proCrp4 molecules occured at the same sites (8). Perhaps the visible MMP-7 cleavage product of (C6A/C21A)-proCrp4 (Fig. 7*A*) represents two or more fragments that remain connected by disulfide bonds. Also, disulfide mutagenesis resulted in more extensive degradation of Crp4 mutants than of the corresponding variant precursors (compare Figs. 5*B* and 7*B*) in that Crp4 cleavage sites corresponding to (Cys/Ala)[83] ↓ Gly[84] and Arg[86] ↓ Phe[87] were not detected at those positions in proCrp4, perhaps because the Crp4 proregion blocks access to those residue positions.

DISCUSSION

The tridisulfide array is a universal and defining feature of the α-defensins (1, 2, 18, 19), but Crp4 bactericidal activity does not require that the array be intact (Figs. 3 and 4). Similarly unanticipated were results showing that Crp4 variants lacking two or three disulfide bonds were more bactericidal against serovar Typhimurium than the parent molecule (Fig. 4). All Crp4 and proCrp4 disulfide mutants were degraded by MMP-7 at several internal positions as determined by N-terminal peptide sequence analysis (Figs. 5*B* and 7*B*), from which we conclude that the disulfide array protects the Crp4 α-defensin moiety during activating proteolysis. Although these studies have focused on the mouse Paneth cell pro-α-defensin processing enzyme (5, 20), similar findings have been observed for corresponding mutations in RMAD-4 and RED-4, myeloid and Paneth cell α-defensins, respectively (21, 22), from rhesus macaque (not shown). We speculate that the disulfide array also may protect α-defensins from degradation in phagolysosomes, after release into the small intestinal lumen or in the extracellular environment at sites of inflammation.

Of the one-, two-, and three-disulfide Crp4 mutants, C6A/C21A adopts the most native-like structure and is the variant most resistant to MMP-7 induced degradation. If C6A/C21A so resembles native structure, why is it susceptible to proteolysis at all when Crp4 is completely resistant? The answer appears to be due to the enhanced molecular flexibility of this mutant relative to Crp4. Evidence for this possibility may be seen in the significantly broadened NMR signals for all of the amide protons in the C6A/C21A mutant relative the native peptide (compare the *upper two* traces in Fig. 2*A*) and in the reduced size of αH secondary shifts (compare the *upper two traces* in Fig. 2*B*). Signal broadening is particularly acute at residues 6–8 and 25–26, and the αH signals for these residues are broadened beyond detection in (C6A/C21A)-Crp4. The enhanced mobility near Cys[6] reflects the removal of a crosslinking disulfide bond and potential disruption of the first strand of the triple-stranded β-sheet, whereas the broadening at Phe[25]-Leu[26] is associated with an extended hairpin turn between the second and third β-strands. This turn appears to be one of the major sites for proteolytic degradation of the mutant peptide with three cleavages occurring nearby, including one directly at the Phe[25]-Leu[26] peptide bond. In the structure of the rabbit kidney α-defensin RK-1 (23), this hairpin turn is relatively solvent-exposed and, by homology, is predicted to be exposed similarly in native Crp4 and more so in

FIG. 7. **MMP-7-mediated proteolysis of proCrp4 disulfide variants.** Samples (11 μg) of proCrp4 mutants (Fig. 1*B*) were incubated overnight at 37 °C in the presence or absence of MMP-7 and analyzed in AU-PAGE and by N-terminal sequence analysis as in Fig. 5. In *panel A*, 11-μg samples of the peptides shown were subjected to analytical acid-urea PAGE with (+) or without (−) incubation with MMP-7 and stained with Coomassie Blue (see "Experimental and Procedures"). *Upper arrow* denotes the position of native proCrp4, *lower arrow* denotes Crp4, and *arrowhead at top* indicates the position of MMP-7. *C6/21A*, C6A/C21A; *C4/11/28/29*, C4A/C11A/C28A/C29A; *6C/A*, C4A/C6A/C11A/C21A/C29A/C29A. In *panel B*, 3-μg samples of proCrp4 and proCrp4 variants incubated overnight with 0.5-mol equivalents of MMP-7 (*panel A*) were analyzed by five cycles of N-terminal peptide sequencing. MMP-7 cleavage sites detected in the Crp4 proregion are depicted by *downward arrows* (↓), and sites within the α-defensin regions of proCrp4 mutants are noted by *inverted triangles* (▼) that interrupt the individual sequences. The α-defensin tridisulfide array is shown above the native proCrp4 sequence and is as predicted for the mutant proCrp4 molecules. Positions at which Cys to Ala mutations occur in Crp4 are shown in *boldfaced type*. Note that MMP-7 does not cleave within the α-defensin region of native proCrp4. Numerals below the (C4A/C6A/C11A/C-21A/C28A/C29A)-proCrp4 sequence (*(all C→A)-proCrp4*) refer to residue positions numbered in relation to the initiating Met position in preproCrp4 as residue number 1. Except for the new site detected in (C4A/C6A/C11A/C21A/C28A/C29A)-proCrp4 (*(all C→A)-proCrp4*) at Gly[84] ↓ Ile[85], the cleavage sites in this sequence are the same as those detected in similar analyses of alkylated proCrp4 (8). *(C6/21A)-proCrp4*, (C6A/C21A)-proCrp4; *(C4/11/28/29A)-proCrp4*, (C4A/C11A/C28A/C29A)-proCrp4.
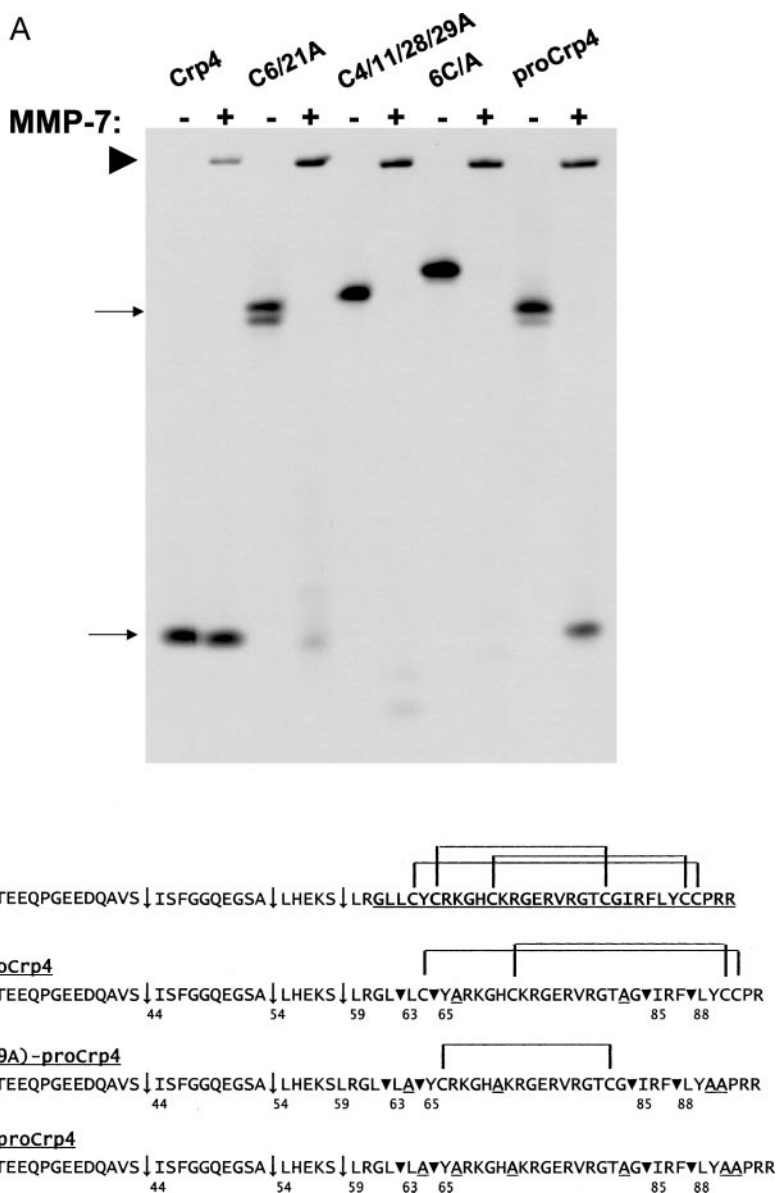
(C6A/C21A)-Crp4, where a disulfide bond that tethers this region to the molecular core is absent. Overall, RK-1 and Crp4 have similarly folded structures (not shown), even though their primary structures are quite different. Relative to Crp4, RK-1 contains two additional residues between Cys[IV] and Cys[V], *i.e.* between strands 2 and 3. Possibly, the structure of the turn between these two strands would be less extended in Crp4 than in RK-1, but residues in the turn still would be solvent-accessible and a major site of proteolytic degradation. The enhanced flexibility of the (C6A/C21A)-Crp4 mutant presumably facilitates access to the enzyme active site, thus increasing the degree of proteolysis.

The disulfide connectivities of Crp4 variants with just a single disrupted disulfide, C4A/29A, C6A/21A, and C11A/28A, were analyzed by MALDI-TOF MS after digestion with MMP-7 (see Fig. 5). For (C11A/C28A)-Crp4, the only disulfide connectivities consistent with the detected peptide masses of 2250.6, 878.0, 3110.4, 1868.2, 3310.9, and 2837.3 atomic mass units are the predicted Cys[I]-Cys[VI] and Cys[II]-Cys[IV] bonds, confirming the correct pairings for this peptide. On the basis of similar findings, we could exclude the possibility of Cys[I]-Cys[III] and Cys[V]-Cys[VI] disulfide pairings in (C6A/C21A)-Crp4 as well as Cys[II]-Cys[III] and Cys[IV]-Cys[V] disulfide bonds in (C4A/C29A)-Crp4,

because no peptide masses consistent with those respective bonding patterns were detected. However, MALDI-TOF MS analysis of (C6A/C21A)-Crp4 MMP-7 digests was unable to distinguish correct Cys[I]-Cys[VI] and Cys[III]-Cys[V] bond pairings from a possible Cys[I]-C[V] and Cys[III]-Cys[VI] folded variant. Similarly, we could not differentiate between correct Cys[II]-Cys[IV] and Cys[III]-Cys[V] connectivities in (C4A/C29A)-Crp4 from a possible Cys[II]-Cys[V] and Cys[III]-Cys[IV] misfolded variant. Thus, in the case of these two mutants, the relation of peptide tertiary structure to activity is uncertain. Nevertheless, the disulfide pairings of (C11A/C28A)-Crp4, (C4A/C11A/C28A/C29A)-Crp4 with a solitary Cys[II]-Cys[IV] bond, and disulfide-null (C4A/C6A/C11A/C21A/C28A/C29A)-Crp4 are unambiguous.

Alterations in the tridisulfide array of β-defensin hBD-3 also have little effect on its microbicidal activity (24). Although α- and β-defensins both have six Cys residues that form specific and invariant disulfide bond pairings (2, 25), the spacing of α- and β-defensin cysteines and their Cys-Cys pairings differ, and they have markedly different precursor structures. The α-defensin cystine connectivities are Cys[I]-Cys[VI], Cys[II]-Cys[IV], and Cys[III]-Cys[V], and the pairings of β-defensins are Cys[I]-Cys[V], Cys[II]-Cys[IV], and Cys[III]-Cys[VI], yet the peptides have similar folded conformations (26–31). Of the six hBD-3 variants with mispaired Cys

connectivities analyzed (32), the microbicidal activities of native hBD-3, mispaired variants, and disulfide-null hBD-3 were the same (24, 32). Similarly, the bactericidal activity of bovine β-defensin BNBD-12 against *E. coli* was also independent of the disulfide array (33). The possible role of β-defensin disulfide connectivities in conferring resistance to proteolysis is unknown to our knowledge, perhaps because the mechanisms of β-defensin posttranslational processing remain obscure.

Studies with model membranes support the view that Paneth cell and myeloid α-defensins kill their targets by permeabilizing the cell envelope, thus leading to dissipation of electrochemical gradients, although the mechanisms of individual peptides often differ (19, 34). Mouse Crp4 induces graded leakage from quenched fluorophore-loaded large unilamellar vesicles (9, 10, 35, 36), and preliminary results show that the Crp4 disulfide variants described here induce large unilamellar vesicle leakage by the same mechanism and at levels corresponding to their relative bactericidal activities.[2] Although the disulfide array has been thought to facilitate peptide-membrane interactions by maintaining a constrained amphipathic β-sheet structure, those interactions clearly are independent of disulfide bonding. Perhaps the disordered, random coil structures of the disulfide variants in aqueous solution (Fig. 2) assume the β-sheet structure of disulfide-stabilized Crp4 when in hydrophobic environments that mimic the lipid-water interface at the membrane surface. Alternatively, in the absence of constraints imposed by the disulfide array, the Crp4 molecule may adopt an unrelated configuration that retains amphipathicity and membrane-disruptive behavior.

Transcripts coding for α-defensins with mutations at disulfide bonds accumulate in mouse small bowel. For example, C57BL/6 mouse small intestine expresses at least 12 α-defensin genes with mutations at varied Cys residue positions. For example, certain mutations are predicted to disrupt the Cys^I-Cys^{VI} disulfide bond, including (C6Y)-Crp (GenBank™ accession number AV070313) and two different (C6F)-Crps (AV-064537 and AV061023). An additional (C6F)-Crp mutant also has an Arg^{35} to Cys substitution that could enable the formation of an alternative Cys^I-Cys^{VI} bond (AV070855). Double mutants of the Cys^I-Cys^{VI} linkage also exist as exemplified by (C1W/C6F)-Crp (AV067626) and (C1S/C6F)-Crp (AV067447). Three different (C5W)-Crp mutant peptides would disrupt the Cys^{III}-Cys^V bond (AV064900, AV070633, and AV066474), and a (C4F)-Crp peptide would lack the Cys^{II}-Cys^{IV} disulfide (AV-065642). In addition to these predicted single disulfide bond disruptions, (C1S/C2S/C3F/C6F)-Crp (AV066139) and (C3F/C-4F/C5S/C6F)-Crp (AV070606) mutants would lack all disulfides typical of α-defensins. Although the actual disulfide connectivities in these deduced Crp mutants are unknown, especially *in vivo*, our findings predict that the α-defensin component of these expressed proforms would be degraded during MMP-7-mediated activation. Given the demonstrated impact of Paneth cell α-defensins on enteric immunity (3), a loss of function caused by MMP-7- or trypsin-mediated proteolysis of naturally occurring α-defensin disulfide mutants could

have adverse consequences for innate immunity in the small intestine.

REFERENCES

1. Ganz, T. (2003) *Nat. Rev. Immunol.* **3,** 710–720
2. Selsted, M. E., and Harwig, S. S. (1989) *J. Biol. Chem.* **264,** 4003–4007
3. Salzman, N. H., Ghosh, D., Huttner, K. M., Paterson, Y., and Bevins, C. L. (2003) *Nature* **422,** 522–526
4. Ayabe, T., Satchell, D. P., Wilson, C. L., Parks, W. C., Selsted, M. E., and Ouellette, A. J. (2000) *Nat. Immunol.* **1,** 113–118
5. Wilson, C. L., Ouellette, A. J., Satchell, D. P., Ayabe, T., Lopez-Boado, Y. S., Stratman, J. L., Hultgren, S. J., Matrisian, L. M., and Parks, W. C. (1999) *Science* **286,** 113–117
6. Ouellette, A. J., Hsieh, M. M., Nosek, M. T., Cano-Gauci, D. F., Huttner, K. M., Buick, R. N., and Selsted, M. E. (1994) *Infect. Immun.* **62,** 5040–5047
7. Selsted, M. E., Miller, S. I., Henschen, A. H., and Ouellette, A. J. (1992) *J. Cell Biol.* **118,** 929–936
8. Shirafuji, Y., Tanabe, H., Satchell, D. P., Henschen-Edman, A., Wilson, C. L., and Ouellette, A. J. (2003) *J. Biol. Chem.* **278,** 7910–7919
9. Satchell, D. P., Sheynis, T., Shirafuji, Y., Kolusheva, S., Ouellette, A. J., and Jelinek, R. (2003) *J. Biol. Chem.* **278,** 13838–13846
10. Satchell, D. P., Sheynis, T., Kolusheva, S., Cummings, J. E., Vanderlick, T. K., Jelinek, R., Selsted, M. E., and Ouellette, A. J. (2003) *Peptides* **24,** 1793–1803
11. Wüthrich, K. (1986) *NMR of Proteins and Nucleic Acids*, pp. 130–161, Wiley-Interscience, New York
12. Lehrer, R. I., Barton, A., and Ganz, T. (1988) *J. Immunol. Methods* **108,** 153–158
13. Selsted, M. E. (1993) *Genet. Eng. (N. Y)* **15,** 131–147
14. Groisman, E. A., Chiao, E., Lipps, C. J., and Heffron, F. (1989) *Proc. Natl. Acad. Sci. U. S. A.* **86,** 7077–7081
15. Fields, P. I., Groisman, E. A., and Heffron, F. (1989) *Science* **243,** 1059–1062
16. Gunn, J. S., Ernst, R. K., McCoy, A. J., and Miller, S. I. (2000) *Infect. Immun.* **68,** 3758–3762
17. Miller, S. I., Pulkkinen, W. S., Selsted, M. E., and Mekalanos, J. J. (1990) *Infect. Immun.* **58,** 3706–3710
18. Lehrer, R. I., Ganz, T., and Selsted, M. E. (1991) *Cell* **64,** 229–230
19. White, S. H., Wimley, W. C., and Selsted, M. E. (1995) *Curr. Opin. Struct. Biol.* **5,** 521–527
20. Ayabe, T., Satchell, D. P., Pesendorfer, P., Tanabe, H., Wilson, C. L., Hagen, S. J., and Ouellette, A. J. (2002) *J. Biol. Chem.* **277,** 5219–5228
21. Tanabe, H., Yuan, J., Zaragoza, M. M., Dandekar, S., Henschen-Edman, A., Selsted, M. E., and Ouellette, A. J. (2004) *Infect. Immun.* **72,** 1470–1478
22. Tang, Y. Q., Yuan, J., Miller, C. J., and Selsted, M. E. (1999) *Infect. Immun.* **67,** 6139–6144
23. McManus, A. M., Dawson, N. F., Wade, J. D., Carrington, L. E., Winzor, D. J., and Craik, D. J. (2000) *Biochemistry* **39,** 15757–15764
24. Hoover, D. M., Wu, Z., Tucker, K., Lu, W., and Lubkowski, J. (2003) *Antimicrob. Agents Chemother.* **47,** 2804–2809
25. Tang, Y. Q., and Selsted, M. E. (1993) *J. Biol. Chem.* **268,** 6649–6653
26. Zimmermann, G. R., Legault, P., Selsted, M. E., and Pardi, A. (1995) *Biochemistry* **34,** 13663–13671
27. Skalicky, J. J., Selsted, M. E., and Pardi, A. (1994) *Proteins* **20,** 52–67
28. Pardi, A., Zhang, X. L., Selsted, M. E., Skalicky, J. J., and Yip, P. F. (1992) *Biochemistry* **31,** 11357–11364
29. Schibli, D. J., Hunter, H. N., Aseyev, V., Starner, T. D., Wiencek, J. M., McCray, P. B., Jr., Tack, B. F., and Vogel, H. J. (2002) *J. Biol. Chem.* **277,** 8279–8289
30. Hoover, D. M., Rajashankar, K. R., Blumenthal, R., Puri, A., Oppenheim, J. J., Chertov, O., and Lubkowski, J. (2000) *J. Biol. Chem.* **275,** 32911–32918
31. Hoover, D. M., Chertov, O., and Lubkowski, J. (2001) *J. Biol. Chem.* **276,** 39021–39026
32. Wu, Z., Hoover, D. M., Yang, D., Boulegue, C., Santamaria, F., Oppenheim, J. J., Lubkowski, J., and Lu, W. (2003) *Proc. Natl. Acad. Sci. U. S. A.* **100,** 8880–8885
33. Mandal, M., Jagannadham, M. V., and Nagaraj, R. (2002) *Peptides* **23,** 413–418
34. Hristova, K., Selsted, M. E., and White, S. H. (1996) *Biochemistry* **35,** 11888–11894
35. Tanabe, H., Qu, X., Weeks, C. S., Cummings, J. E., Kolusheva, S., Walsh, K. B., Jelinek, R., Vanderlick, T. K., Selsted, M. E., and Ouellette, A. J. (2004) *J. Biol. Chem.* **279,** 11976–11983
36. Cummings, J. E., Satchell, D. P., Shirafuji, Y., Ouellette, A. J., and Vanderlick, T. K. (2003) *Aust. J. Chem.* **56,** 1031–1034

[2] J. E. Cummings, T. K. Vanderlick, A. J. Ouellette, unpublished data.

Functional Analysis of the α-Defensin Disulfide Array in Mouse Cryptdin-4

Atsuo Maemoto, Xiaoqing Qu, K. Johan Rosengren, Hiroki Tanabe, Agnes
Henschen-Edman, David J. Craik and Andre J. Ouellette